American Journal of Pathology, Vol. 138, No. 1, January 1991

Cortical and Subcortical Patterns of Synaptophysinlike Immunoreactivity in Alzheimer's Disease

Eliezer Masliah, Robert D. Terry, Michael Alford, Richard DeTeresa, and Lawrence A. Hansen

From the Department of Neurosciences, University of California, San Diego, School of Medicine, La Jolla, California

Quantification of synaptophysinlike immunoreactivity is a valuable method for studying the presynaptic terminals in the normal and damaged nervous system. The present report shows that in the control brain, the predominant pattern of synaptic immunostaining in the neocortex was that of an evenly distributed densely granular immunolabeling of the neuropil, while in the paleocortex and in subcortical areas of the brain most of the presynaptic terminals were distributed along the dendritic arborizations or around the neuronal somata. The immunochemical and the immunohistochemical analysis of the Alzheimer's disease tissue showed that the frontal and parietal cortex presented the most severe and widespread loss, with a 45% loss in synaptophysin immunoreactivity. These areas showed an average 35% loss of large neurons. The visual cortex, hippocampus, entorhinal cortex, nucleus basalis of Meynert, and locus ceruleus displayed some degree of loss, but to a lesser extent. In addition to this loss, the basic patterns of organization of the presynaptic terminals were altered, with the presence of abundant, enlarged synaptophysin-labeled terminals. This study further supports the role of synaptic pathology in Alzheimer's disease. (Am J Pathol 1991, 138:235–246)

Quantification of synaptophysinlike immunoreactivity is a valuable method for evaluating the status of the central nervous system presynaptic terminal populations in normal and pathologic conditions.[1,2] Previous work with this method showed significant synaptic loss in the Alzheimer's disease (AD) neocortex[3] and in the molecular layer of AD hippocampus.[4] Studies comparing patterns of synaptophysinlike immunoreactivity in other areas of AD brains and the normal aged brain have not yet appeared. It also remains to be determined whether synapse loss is a consequence of the retrograde or anterograde degeneration induced by cortical damage, and the extent to which synaptic loss relates to neuronal loss. The present report 1) compares the degree of presynaptic terminal loss in cortical and subcortical regions of AD brain, and describes the synaptic organization demonstrated by synaptophysinlike immunoreactivity; 2) compares presynaptic terminal loss with neuronal loss in different neocortical areas; and 3) provides further quantitative immunochemical data obtained by Western blot analysis of control and AD nervous system tissue, immunoreacted with the monoclonal antibody (SY38) against the presynaptic terminal vesicle protein synaptophysin[5] (p38).[6]

Materials and Methods

Samples

Ten autopsy cases from the Alzheimer's Disease Research Center at the University of California, San Diego, were used in the present study. Five of these cases had clinical AD that was confirmed at autopsy histopathologically. The average age of the AD cases was 75 ± 6 years, with a postmortem delay of 5.4 ± 1.2 hours. The other five cases were clinically and pathologically free of neurologic disease. The average age of these control cases was 72 ± 13 years, with a postmortem delay of 6 ± 1.6 hours. In each case, the right hemibrain was frozen at −70°C for further immunochemical and biochemical analyses. The left hemibrain was fixed in 4% buffered formalin for 5 days to preserve the relative antigenicity of the tissue[2] because prolonged fixation has been shown

Supported by National Institutes of Health grants AGO8201 and AGO5131 and the PEW Charitable Trust. Eliezer Masliah has a fellowship from NIH Training Grant NS-07078.

Accepted for publication September 6, 1990.

Address reprint requests to Dr. Eliezer Masliah, Department of Neurosciences, University of California, San Diego, School of Medicine, M-024, La Jolla, CA 92093.

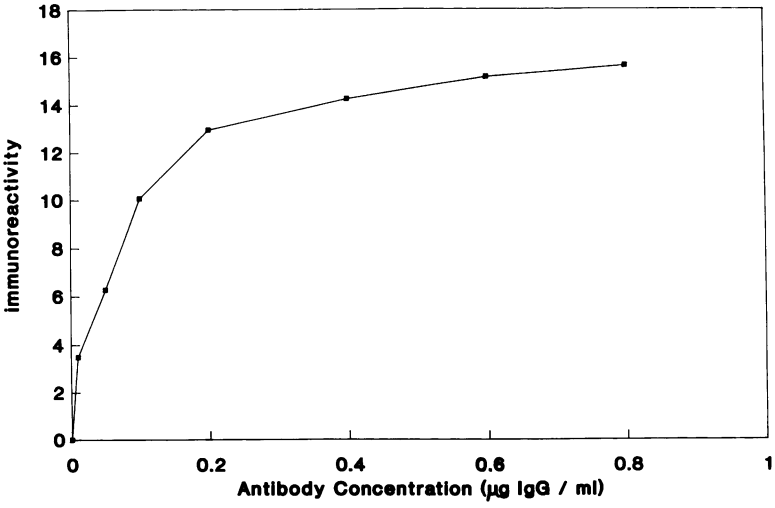

Figure 1. *Effect of antibody concentration on synaptophysin immunoreactivity (38-kd band) from homogenates of human frontal cortex. The protein concentration per lane was 25 µg. The saturation and half-saturation points (determined by double-reciprocal plot) were reached at concentrations of anti-synaptophysin (SY38) of 1.5, and 0.09 µg/ml, respectively. The usable antibody concentration range was from 0.05 to 0.2 µg/ml. The integrated optical density of the immunoreactive band in the Western blot is plotted as immunoreactivity on the y axis.*

to alter synaptophysin immunohistochemical demonstrability.[7] In each of the 10 cases, blocks were taken (as defined elsewhere[8]) from the midfrontal (MF), inferior parietal (IP), superior temporal (ST), and striate (areas 17 and 18) neocortex, posterior and anterior hippocampus/entorhinal cortex, basal ganglia, nucleus basalis of Meynert (NbM), cerebellum, mesencephalon (at the level of the oculomotor nucleus), and pons (at the level of the locus ceruleus). The thalamus and olfactory system, because of their neuroanatomic complexity, were not included in this report and will be the subject of another study. The tissue blocks were dehydrated, paraffin embedded, and 5-μ-thick paraffin sections were mounted onto triple-coated gelatin-alum slides.

Immunohistochemistry

Briefly, as previously described,[2,3] reproducible results were obtained by incubating the sections at 4°C overnight with the monoclonal antibody SY38 against synaptophysin[5] (Boehringer Mannheim Laboratories, Indianapolis, IN; 4 µg/ml), followed by incubation in biotinylated horse anti-mouse (Vector 1:100) and Avidin-D-HRP (Vector Laboratories, Burlingame, CA; ABC Elite 1:75). The reaction was visualized by developing the sections in 40 mg of diaminobenzidine in 100 ml of 0.1 TRIS–HCL containing 45 µl of H_2O_2 (30%) for 15 minutes. All sections were treated simultaneously under the same conditions. The immunolabeling protocol was repeated twice in adjacent 5-μ-thick paraffin sections to assure reproducibility of results.

Microdensitometry and Morphometry

Anti–synaptophysin-immunostained sections from the MF, IP, ST, and striate (areas 17 and 18) cortex were studied with the Cambridge 970 Quantimet (Cambridgde Instru-

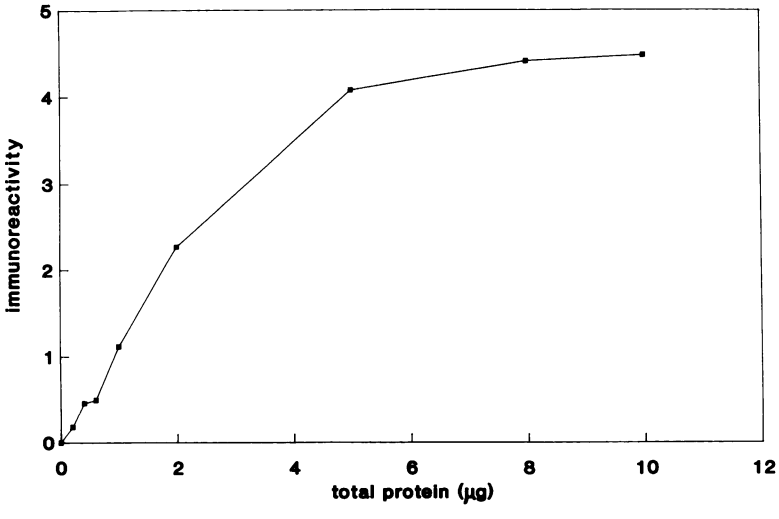

Figure 2. *Effect of total protein concentration from human frontal cortex homogenate on anti-synaptophysin immunoreactivity. Primary antibody was used at a concentration of 0.1 µg/ml; nonlinearity became apparent at a concentration of more than 4 µg total protein. The ideal range of protein concentration was from 1 to 2 µg total protein. The integrated optical density of the immunoreactive zone in the dot blot is plotted as 'immunoreactivity' on the y axis.*

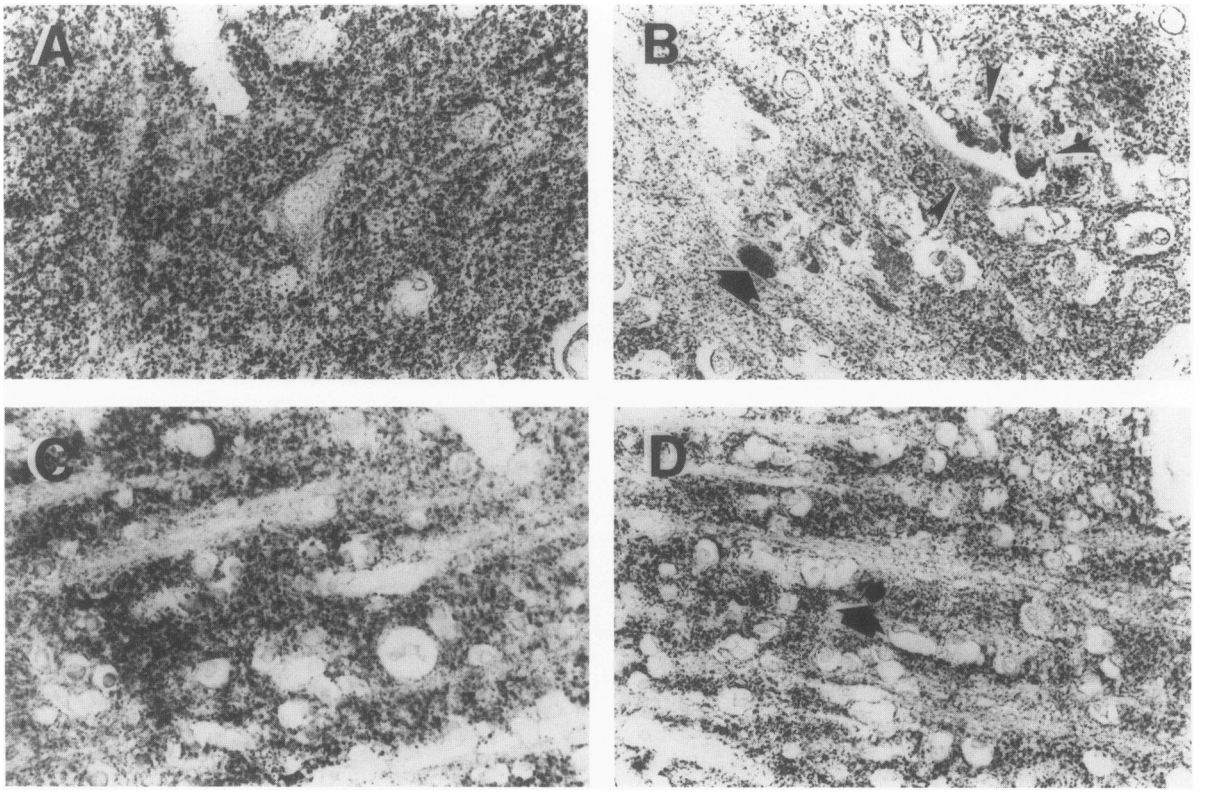

Figure 3. *Synaptophysinlike immunoreactivity in the human neocortex.* **A:** *Layer III of the control frontal cortex displayed dense granular immunostaining.* **B:** *The AD frontal cortex showed a significant decrease in immunoreactivity accompanied by strongly reacting dystrophic neurites in the neuropil (solid arrow) and around degenerating neurons (arrow heads).* **C:** *Layer IV of the control visual cortex (area 17) presented dense immunolabeling.* **D:** *In contrast, the AD visual cortex displayed a 25% decrease in immunoreactivity as well as the presence of abnormal terminals (arrow) (×264).*

ments, UK) as previously described.[2] The optical density (OD) of the reaction product in the neuropil of layers II to V was measured and averaged. The same method was used to quantify the immunoreactivity of the outer and inner molecular layers of the dentate gyrus of the hippocampus. The OD of the white matter in each section was subtracted to arrive at a corrected value (COD). Total cell counts (glia, large and small neurons) were performed with the Quantimet 970 in 20-μ-thick cresyl violet-stained sections of the MF, IP, and ST as previously described.[8] Photomicrographs (Figures 3 and 5 to 12) of individual fields in each comparison group were taken and processed under identical conditions.

Table 1. *Loss of Neurons and Presynaptic Terminals in AD Midfrontal Cortex*

Synaptophysinlike immunoreactivity (corrected OD)§	Alzheimer disease (n = 5)	Control (n = 5)	% Loss
Layer II	110 ± 32*	206 ± 13	−47
Layer III	123 ± 42†	219 ± 10	−44
Layer IV	128 ± 37‡	192 ± 5	−34
Layer V	137 ± 50‡	233 ± 13	−42
Large neuron counts (>90 μ)§	258 ± 99	380 ± 103	−33
Small neuron counts (40–90 μ)§	819 ± 112	729 ± 159	+11

AD, Alzheimer's disease; OD, optical density.
* $P < 0.001$.
† $P < 0.002$.
‡ $P < 0.01$.
§ Mean ± SD.

Table 2. *Loss of Neurons and Presynaptic Terminals in AD Inferior Parietal Cortex*

Synaptophysinlike immunoreactivity (corrected OD)*	Alzheimer disease (n = 5)	Control (n = 5)	% Loss
Layer II	119 ± 33†	250 ± 15	−53
Layer III	124 ± 43†	278 ± 18	−56
Layer IV	114 ± 30†	232 ± 20	−51
Layer V	120 ± 43†	289 ± 20	−59
Large neuron counts (>90 μ)*	246 ± 119	364 ± 91	−41
Small neuron counts (40–90 μ)*	887 ± 204	854 ± 189	+4

AD, Alzheimer's disease; OD, optical density.
* Mean ± SD.
† $P < 0.001$.

Table 3. *Loss of Neurons and Presynaptic Terminals in AD Superior Temporal Cortex*

Synaptophysinlike immunoreactivity (corrected OD)*	Alzheimer disease (n = 5)	Control (n = 5)	% Loss
Layer II	151 ± 27‡	231 ± 27	−35
Layer III	150 ± 22†	246 ± 25	−40
Layer IV	147 ± 12†	232 ± 20	−37
Layer V	154 ± 36†	256 ± 19	−40
Large neuron counts (>90 μ)*	282 ± 134	410 ± 66	−32
Small neuron counts (40–90 μ)*	843 ± 156	796 ± 166	+6

AD, Alzheimer's disease; OD, Optical density.
* Mean ± SD.
† $P < 0.001$.
‡ $P < 0.002$.

Immunochemical Detection and Quantification

To determine optimal incubation conditions with respect to concentrations of primary antibody (SY38, anti-synaptophysin) and brain homogenate protein for immunochemical quantitative studies, preliminary Western blot and dot blot analyses were performed on whole frontal cortex homogenates from a typical control case. Total protein was quantified by the method of Lowry et al[9] and by a modified Peterson microassay method.[10] Multiple dilutions of primary antibody (Figure 1) were tested on a blot of uniform protein concentration using a multilane miniblotter (Immunetics, Cambridge, MA). A dot blot was used to assess the effect of protein concentration (Figure 2). Working concentrations were chosen empirically from results that fell within a linear range while showing minimal nonspecific binding profiles.

Brain homogenates from the right frontal cortex of five control and five AD cases were separated into particulate and cytosolic fractions as previously described.[11] Sodium dodecyl sulfate–polyacrylamide gel electrophoresis (SDS-PAGE) and Western blotting were performed according to the methods of Laemmli[12] and Towbin,[13] respectively. Briefly, 1.4 μg of total protein (Figure 1) per well of each fraction (from each case) were electrophoresed on 10% SDS polyacrylamide gels (pH 8.8), blotted to nitrocellulose, and blocked for 2 hours with 0.1% Tween 20 in phosphate-buffered saline (TPBS). Blots were incubated with mouse monoclonal anti-synaptophysin at a concentration of 0.1 μg/ml (PBS, 3% bovine serum albumin [BSA], pH 7.4) (Figure 2) for 36 hours at 4°C, followed by rabbit anti-mouse IgG (Accurate Chemical and Scientific Corp. New York, NY) at 0.85 μg/ml (PBS-BSA) for 2 hours at 4°C, followed by ^{125}I-protein A (0.5 Ci/ml, PBS-BSA) for 2 hours at 4°C.

Blots were autoradiographed on RPX-omat film in cassettes with Dupont CRONEX intensifying screens. Special care was taken with regard to film exposure to ensure an OD between 0.8 and 2.5, where film response is relatively linear. The autoradiographs were scanned using a Phar-

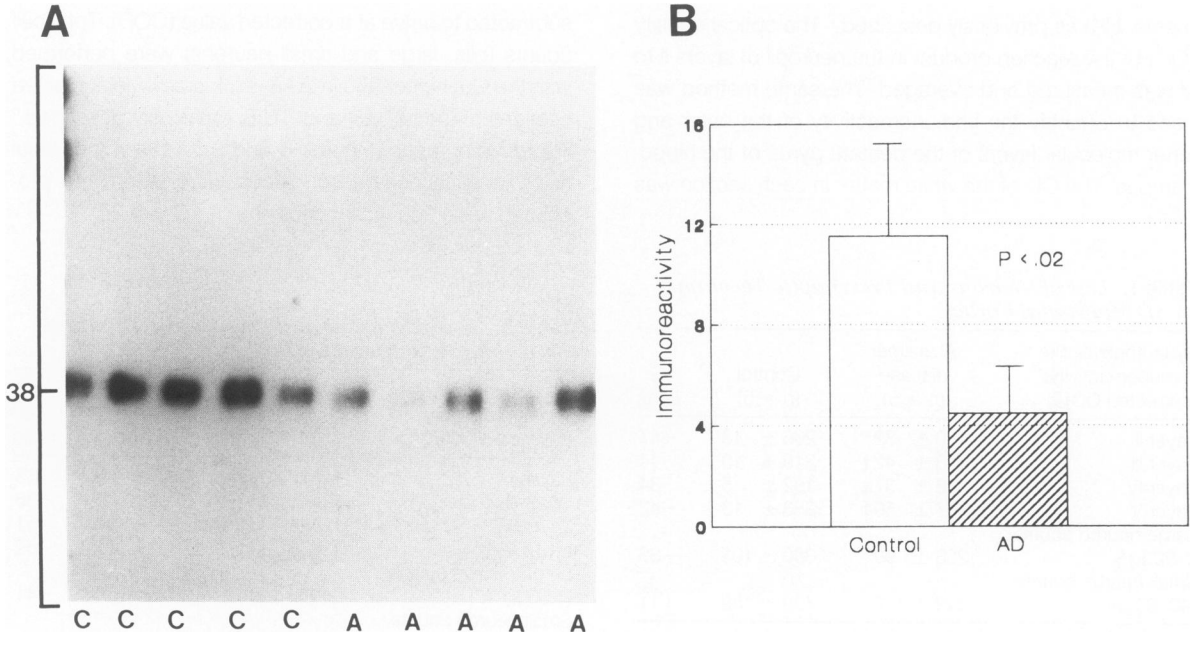

Figure 4. *Synaptophysin immunodetection by Western blot analysis of the particulate fraction of the frontal cortex.* **A:** *Anti-synaptophysin detected a broad band with an apparent molecular weight of 38 kd. C = controls, A = Alzheimer.* **B:** *Immunoquantification of the Western blot shows a significant decrease in synaptophysin immunostaining in AD. Bars are SEM. n = 5 controls, n = 5 AD cases. The integrated optical density of the immunoreactive band in the Western blot is plotted as 'Immunoreactivity' on the y axis.*

macia LKB Ultrascan laser densitometer (Pharmacia, Upsalla, Sweden) for quantification of the 38-kd band. Areas under peaks were determined by digital integration using the Quantimet 970 and expressed in pixels. The integrated OD of the immunoreactive band in the Western blot was plotted as 'Immunoreactivity' in the y axis (Figure 4).

Results

Neocortex

The synaptophysinlike immunostained neuropil of frontal, parietal, and temporal cortex displayed a characteristic granular pattern with densest reactivity in layers II, III, and V (Figure 3A, Tables 1 to 3). The AD samples from these areas showed an average 45% ± 8% decrease in immunoreactivity (Tables 1 to 3), probably relating to a decrease in the number of immunolabeled presynaptic terminals (Figure 3B). These same AD cases showed average 35% ± 4% loss of large neurons (Tables 1 to 3).

Table 4. *Semiquantitative Assessment of the Synaptophysinlike Immunoreactivity in the IML and OML of the Hippocampus and of the Neuronal Population of the Entorhinal Cortex in AD*

Case	IML density*	OML density*	Entorhinal cortex population†
1	+4	−1	−4
2	+2	−2	−4
3	+4	+1	−2
4	+3	+1	−3
5	+4	−1	−2

IML, inner molecular layer; OML, outer molecular layer; AD, Alzheimer's disease.

* Semiquantitative scoring of the synaptophysin immunostaining density—IML: +4 = intense increase, +3 = moderate increase, +2 = normal level; OML: +3 = intense increase, +2 = moderate increase, +1 = normal level, −1 = mild decrease, −2 = moderate decrease.

† Semiquantitative scoring of the neuronal population in nissl and thioflavine-S stained sections—−4 = intense loss, −3 = moderately intense loss, −2 = moderate loss, −1 = mild loss.

In addition, the AD sections demonstrated immunostained, abnormally dilated neurites scattered in the neuropil and in neuritic plaques (Figure 3B) in layers III and V. The striate neocortex presented a laminar immunolabeling pattern

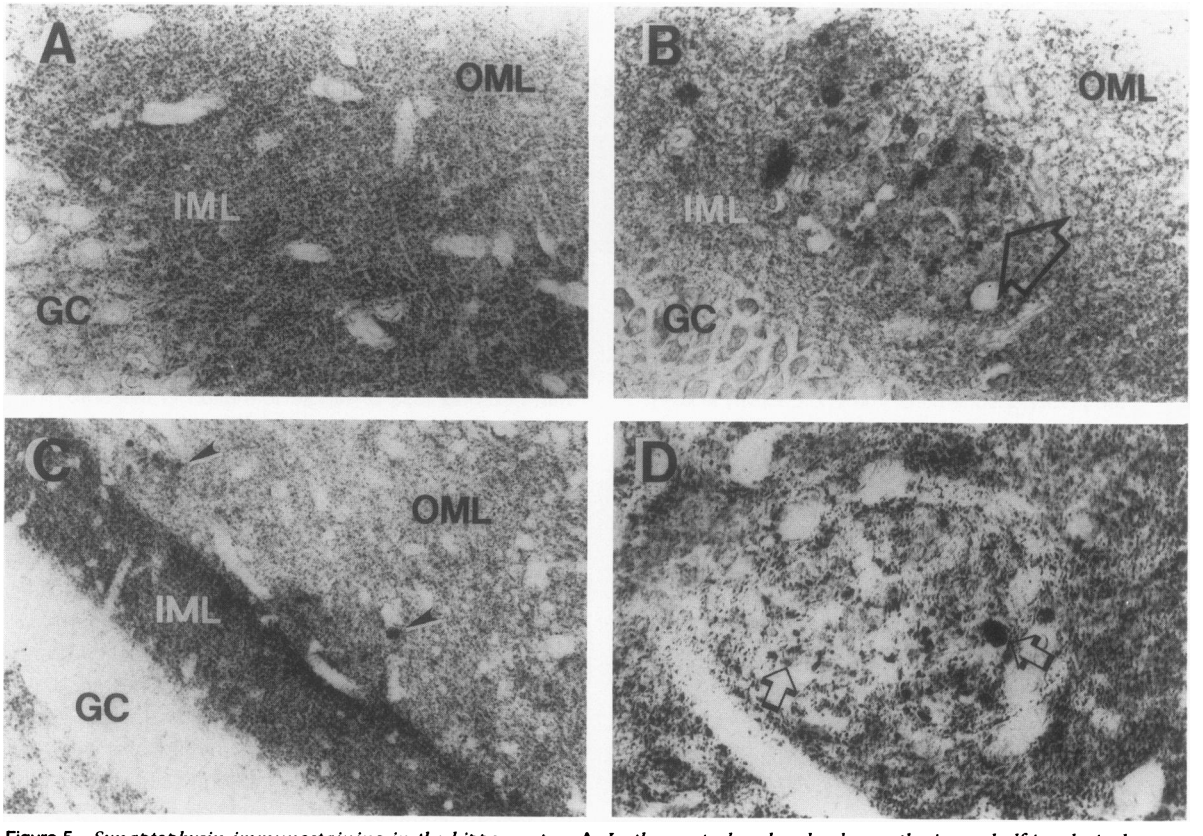

Figure 5. *Synaptophysin immunostaining in the hippocampus.* **A:** *In the control molecular layer, the inner half is relatively more dense than the outer half (×264).* **B:** *In AD some cases displayed a widespread decrease in immunoreactivity in the molecular layer. In addition neuritic plaques (open arrow) with large synaptophysinlike immunoreacting terminals were found in the IML (×264).* **C:** *Other AD cases showed increased immunoreactivity in the IML and scattered dystrophic neurites (arrow heads) in the OML (×264).* **D:** *The subiculum presented neuritic plaques with synaptophysinlike immunolabeled abnormal terminals of different sizes (arrows) (×328). GC, granular cells; IML, inner molecular layer; OML, outer molecular layer.*

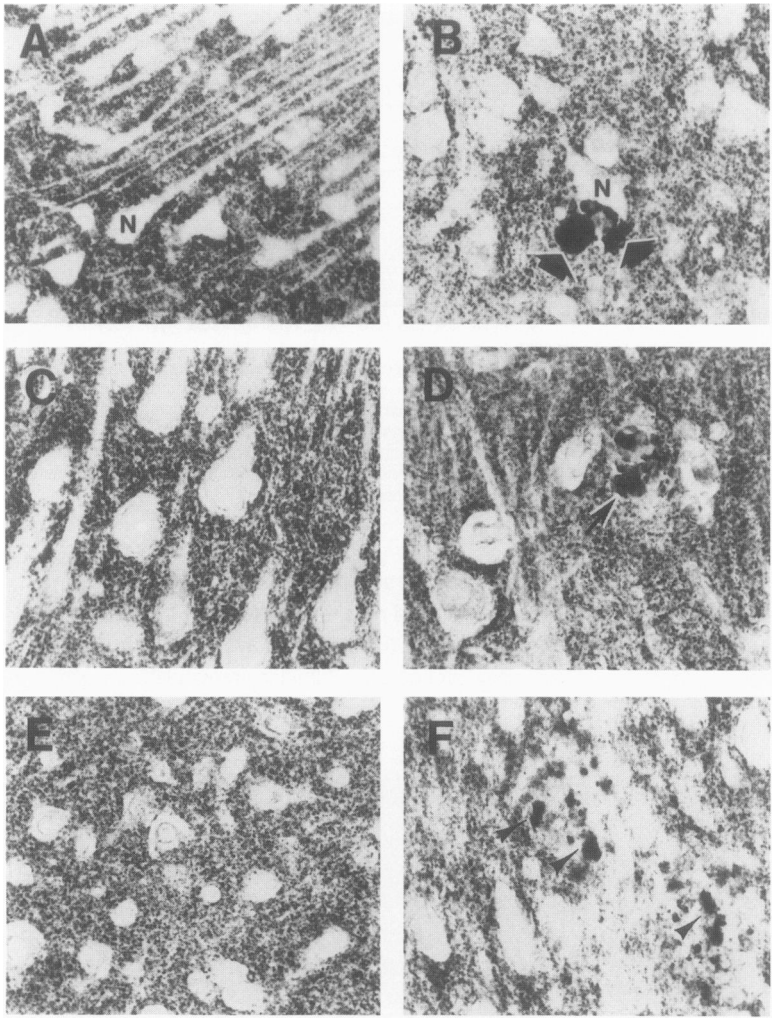

Figure 6. *Synaptophysin immunoreactivity of the cornus Ammonis.* **A:** *The control CA3 area presented a very dense labeling of the neuropil, with negative neuronal cell bodies (N) (×145).* **B:** *The AD CA3 zone displayed some decreased immunoreactivity in the neuropil and enlarged terminals (solid arrows) around the pyramidal neurons (N) (×145).* **C:** *Control CA1 area (×230).* **D:** *AD CA1 presented immunoreacting plaques (arrow) (×230).* **E:** *Control layer III of the parahippocampal gyrus (×145).* **F:** *In AD there were focal areas of decreased immunoreactivity with abnormal neurites in the neuropil (arrow heads) (×145).*

with the densest staining in layer IV of area 17 (Figure 3C and D). Alzheimer's disease area 17 was decreased by 25% in the presynaptic terminal immunoreactivity in layers II, III, and V and by 7.5% in layer IV. In area 18, the AD cases displayed a 15% decrease in the COD.

Western blot analysis of the frontal cortex homogenates showed that the monoclonal antibody against synaptophysin recognized a single band of 38 kd (Figure 4A), 99% detected in the particulate fraction. Consistent with the immunohistochemical studies, the AD samples of the frontal cortex displayed a 60% reduction of the immunoreactivity of the 38-kd band (Figure 4B).

Hippocampus and Entorhinal Cortex

The control molecular layer (ML) of the hippocampal dentate gyrus displayed a poorly delineated bilaminar pattern of immunostaining with denser immunoreactivity in the inner molecular layer (Figure 5A). The AD samples showed a trend toward decreased synaptophysin immunoreactivity in the outer ML, which did not, however, correlate directly with neuronal loss or tangle formation in the entorhinal cortex (Table 4). The inner ML displayed a moderate increase in synaptophysinlike immunoreactivity (Figure 5C). A prominent feature of the ML of all AD cases was the presence of anti-synaptophysin-immunolabeled abnormally dilated neurites in association with senile plaques (Figures 5B to D). The CA4 area of the control hippocampus presented typical strongly immunoreacting individual terminals distributed along dendritic trees (mossy fibers) of pyramidal neurons. In contrast, CA3, CA2, and CA1 areas displayed a very densely populated neuropil (Figures 6A and C). The basic patterns of immunostaining were preserved in the AD cases, although in some instances the cornus ammonis showed focal areas of decreased synaptophysin immunoreactivity (Figures 6B and D) and dilated neurites scattered in the neuropil (Figure 6D). These dystrophic terminals were larger than the ones observed in the neocortex, and some of them were distributed

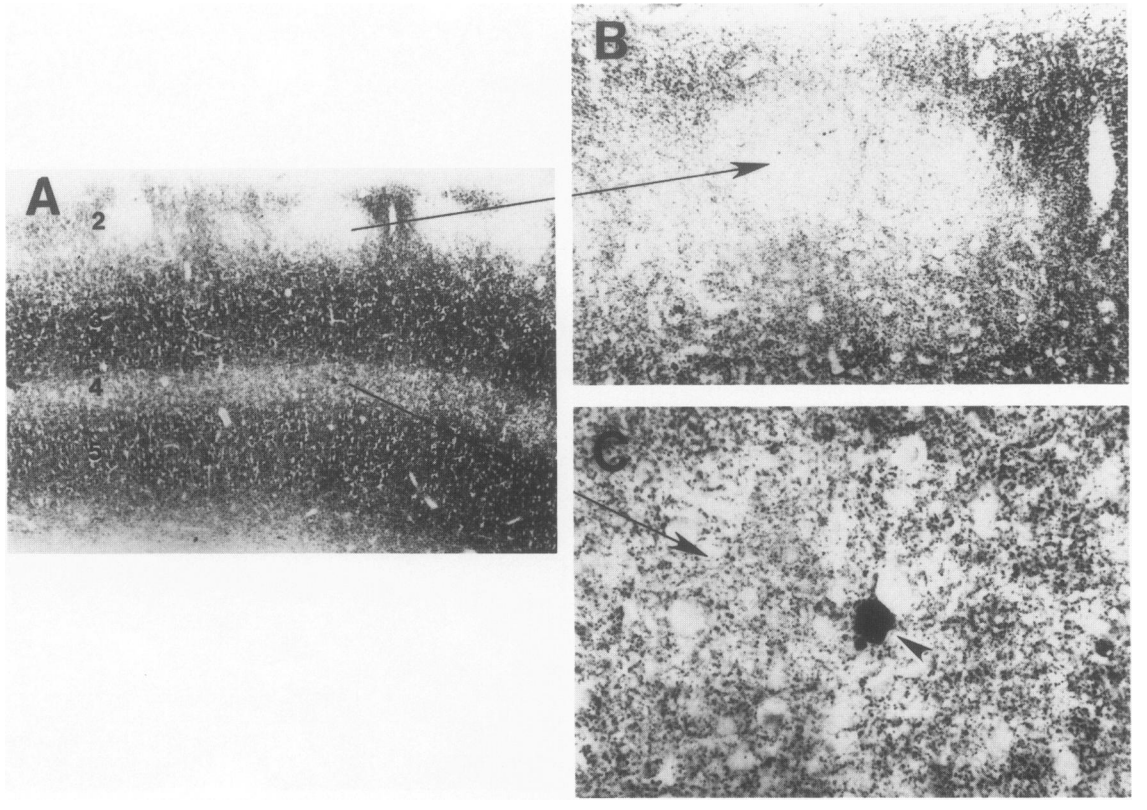

Figure 7. *Synaptophysin immunostaining of the AD entorhinal cortex.* **A:** *A low-power view of the entorhinal cortex revealed laminar staining with denser reaction in layers III and V and lighter reaction in layers II and IV (×20).* **B:** *The glomerate layer displayed a relative decrease in immunostaining (×100). Thioflavin-S revealed abundant tangles in this zone.* **C:** *Layer IV showed a moderate decrease in immunoreactivity accompanied by abnormal dilated neurite (arrow heads) (×100).*

around the perikarya of pyramidal neurons (Figure 6B). The control entorhinal cortex displayed a typical laminar arrangement of presynaptic terminals with decreased immunolabeling in layer II, and in the border between layers IV and V. In contrast, layers III, V, and VI showed denser immunostaining (Figure 6E).

The entorhinal cortex in one AD case showed a significant loss of granular labeling around the nests of neurons in the glomerate layer (lamina II) (Figures 7A and B). Layers III, V, and VI did not show any substantial decrease in synaptophysin immunoreactivity, although all cases displayed abundant dystrophic immunoreacting terminals scattered in the neuropil or surrounding plaques (Figure 6F). Only layer IV presented a moderate decrease in immunoreactivity.

Basal Ganglia and Nucleus Basalis of Meynert

The control caudate and putamen displayed an evenly distributed, densely granular immunostaining pattern in the neuropil (Figures 8A and C) with a 12% higher density in the caudate. Immunostaining density of AD caudate and putamen was similar to those of the control samples, with the exception that in the AD tissue a moderate number of immunoreacting dilated terminals was found (Figures 8B and D). The globus pallidus displayed a pattern completely different from the caudate and putamen. That is, rather than the evenly distributed granular neuropil pattern seen with anti-synaptophysin in the striatum, most of the terminals observed in the globus pallidus were aligned along the dendrites (Figure 9A). Significant differences from controls were not observed in the AD globus pallidus (Figure 9B).

The control NbM presented an immunostaining pattern less dense than other subcortical nuclei. Some of the immunoreacting grains were located around the neuronal somata and others were distributed along dendritic arbors in the neuropil (Figure 9C). The AD NbM had a significant decrease in density of both types of immunoreacting granules (Figure 9D).

Brainstem and Cerebellum

The control substantia nigra displayed two different patterns of synaptophysinlike immunoreactivity. In the pars

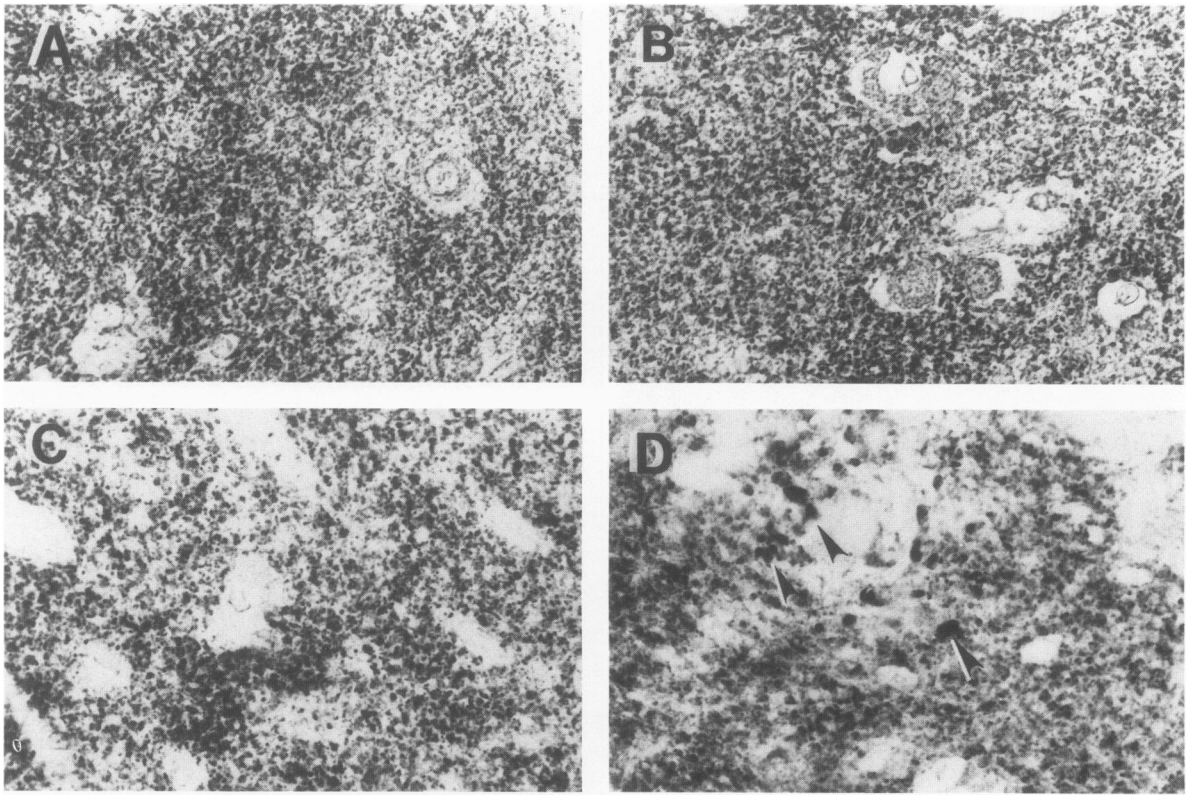

Figure 8. *Synaptophysin immunoreactivity in the basal ganglia.* **A:** *The control caudate nucleus displayed a dense neuropil labeling.* **B:** *The AD samples showed staining intensity similar to the controls.* **C:** *Control putamen.* **D:** *In AD the immunostaining density of the neuropil was similar to control putamen, although some abnormal terminals were found (arrow heads) (×230).*

reticularis, most of the immunolabeled grains were distributed along dendritic trees (Figure 11A) of nonpigmented neurons. In contrast, the presynaptic terminals in the pars compacta also were located around the melanin-containing neurons (Figure 10A), as well as in a low-density granular pattern in the neuropil. This latter pattern of immunoreactivity also was found in the locus ceruleus (Figure 10C). The oculomotor nucleus showed densely labeled individual nerve terminals distributed in the neuropil (Figure 11C). The pontine nucleus presented a typical pattern of synaptophysin immunostaining with a granular, densely populated neuropil (Figure 11D). There were no significant differences in the immunoreactivity patterns between AD and controls in the substantia nigra (Figure 10B), oculomotor nucleus, or pontine nucleus. The AD locus ceruleus displayed a decrease in the number of immunolabeled neuropil grains (Figure 10D).

The control cerebellar vermis displayed fine granular labeling of the molecular layer, with dense immunostaining of prominent terminals around the Purkinje cells, and strongly labeled glomerular synaptic complexes in the inner granular layer (Figure 12A). The AD cerebellum (Figure 12B) presented a mild collapse of the molecular layer, but there was no change in the basic patterns of immunostaining as compared to controls (Figure 12A).

Discussion

Previous quantitative electron microscopic studies in AD biopsy[14] tissue from the frontal cortex have shown a 27% synapse loss in layer V and a 36% synaptic decrease in layer V of the temporal cortex. Electron microscopic studies in autopsy material[15] from AD cases demonstrated a 42% synaptic loss in layers II and III and 29% synapse loss in layer V of the frontal cortex. The present report indicates that in AD the frontal and parietal cortex show the most widespread and severe presynaptic terminal loss, with an average 45% decrease in synaptophysin immunoreactivity. These latter quantitative immunohistochemical results are supported by Western blot analysis and by recent immunochemical and immunohistochemical studies with the membrane skeletal protein—brain spectrin, where increased immunoreactive degradation products are indicators of synapse and neuronal degeneration.[16] The visual cortex, hippocampus, and entorhinal cortex also displayed some synapse loss, but only focally and to a lesser extent. In contrast, areas such as basal ganglia[17] and cerebellum, which are known not to be severely affected in AD, were not marked by a substantial terminal loss. Only in the NbM and locus ceruleus was there significant synaptic decrease. These findings are

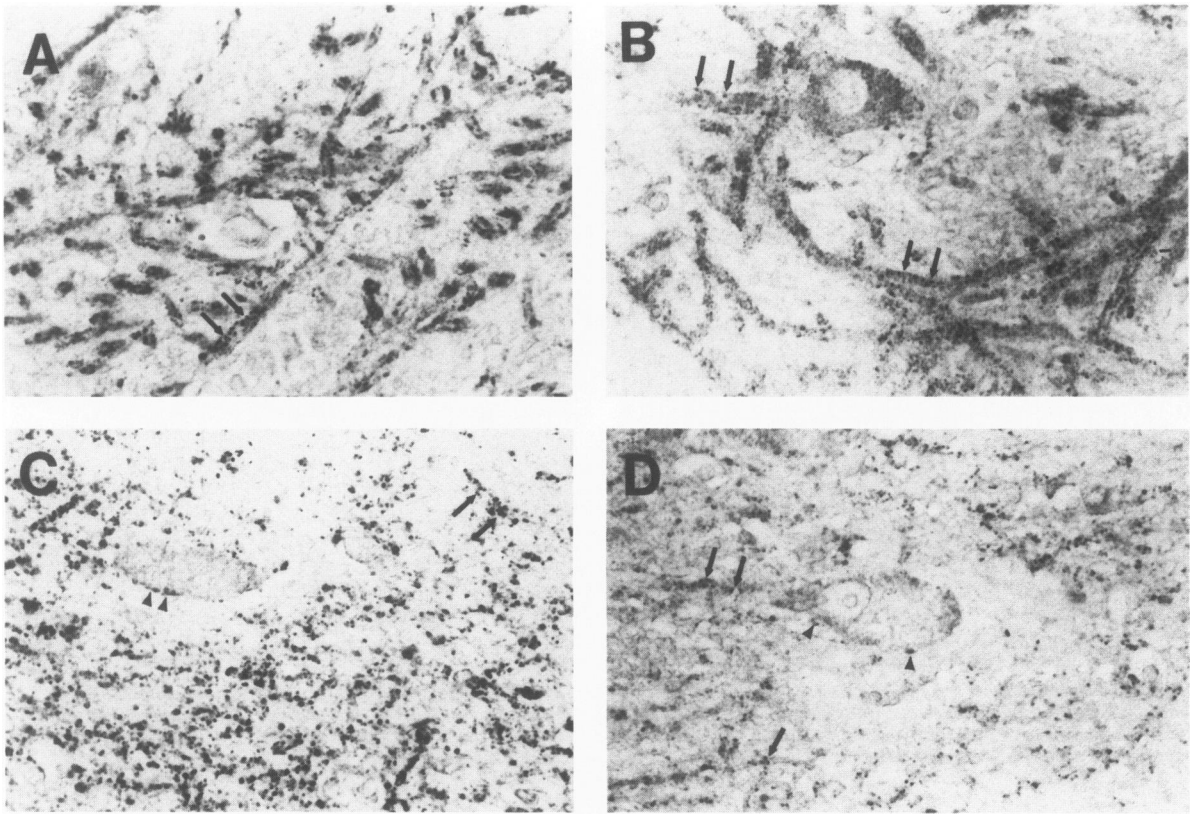

Figure 9. **A:** *The control globus pallidus presented a characteristic granular immunolabeling around dendrites (arrows).* **B:** *The AD globus pallidus presented a preserved immunostaining pattern around the dendrites.* **C:** *The control NbM showed immunostained presynaptic terminals around the cell bodies of neurons (arrow head) as well as scattered in the neuropil (arrows).* **D:** *The AD NbM displayed a moderately severe decrease in immunolabeled nerve terminals (×265).*

consistent with our previous report[3] and support the idea that AD is characterized by extensive presynaptic terminal loss, especially in the neocortex.

The possibility that these immunohistochemical findings in AD neocortex are the results of fixation or postmortem delay rather than specific damage to presynaptic terminals is unlikely because 1) the decreased immunostaining was found in specific areas of the neocortex rather than as a diffuse and widespread loss, 2) the immunohistochemical findings in the neocortex were paralleled by the results of Western blot analyses (of unfixed tissue), 3) the various patterns of immunostaining in different cortical and subcortical regions were consistent with the synaptic distributions reported in previous electron microscopic[18–21] and immunohistochemical studies,[2] and 4) the immunostaining densities observed in the basal ganglia were consistent with previous immunochemical[22] and immunohistochemical studies.[23,24] Our confidence in the ability of this method to quantify synapse loss is bolstered further by the finding of time-dependent changes in synaptophysin immunoreactivity in denervated molecular layer of the rat with unilateral transection of the perforant pathway,[25] as predicted by electron microscopic studies.[26]

The mechanisms underlying synapse loss in the AD neocortex are largely unknown, but possible explanations include 1) presynaptic terminal loss is secondary to neocortical and subcortical (eg, NbM) neuronal loss, or 2) the diminution in synapses in AD is a primary pathologic process due to an agent (or agents) damaging synapses or altering biochemical pathways involved in the maintenance and regulation of synapses and neurons. Peptides related to the amyloid precursor protein may well play a role in this latter hypothesized pathogenesis because one investigation demonstrated that the amyloid beta protein enhances survival of hippocampal neurons *in vitro*.[27] Abnormal processing of the precursor protein could result in a deficiency of this trophic effect causing synaptic loss. Meanwhile other studies showed that different fragments of the amyloid beta protein precursor are involved in the regulation of fibroblasts[28] and have neurotoxic effects on hippocampal neurons *in vitro*.[29]

As to the possible biochemical pathways involved in synapse and neuronal maintenance that could be altered in AD, it was shown that protein kinase C plays an important role in long-term potentiation[30] and synapse modulation.[31] In AD, brain levels of this kinase are reduced,[32] and subtypes alpha, beta I, and beta II are present in the

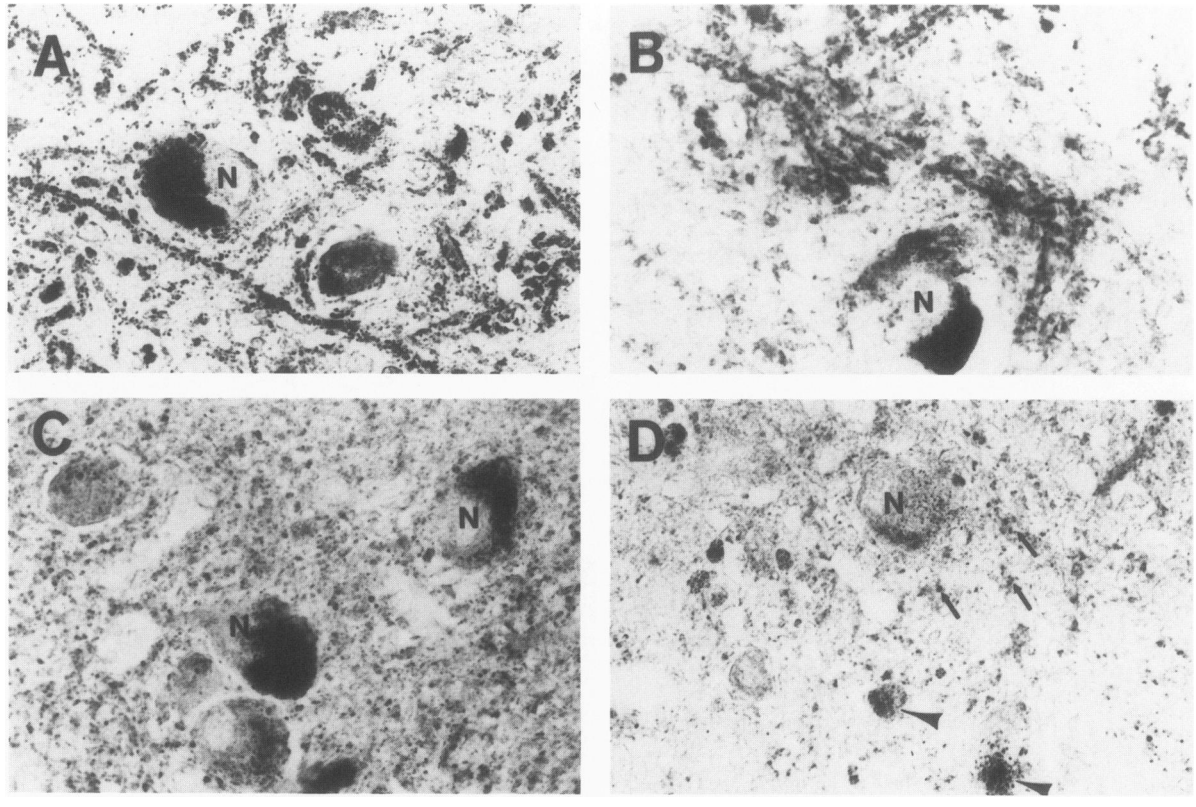

Figure 10. *Synaptophysin immunostaining in the brain stem. Control* **(A)** *and AD* **(B)**. *In the pars compacts of the substantia nigra, immunolabeled synapses were distributed along dendrites with fewer around the pigmented neurons (N). Significant and consistent differences were lacking. Control* **(C)** *and AD* **(D)** *locus ceruleus. In AD there was a decreased number of perineuronal (N) and neuropil presynaptic terminals (arrows). The arrow heads indicate extraneuronal melanin (×265).*

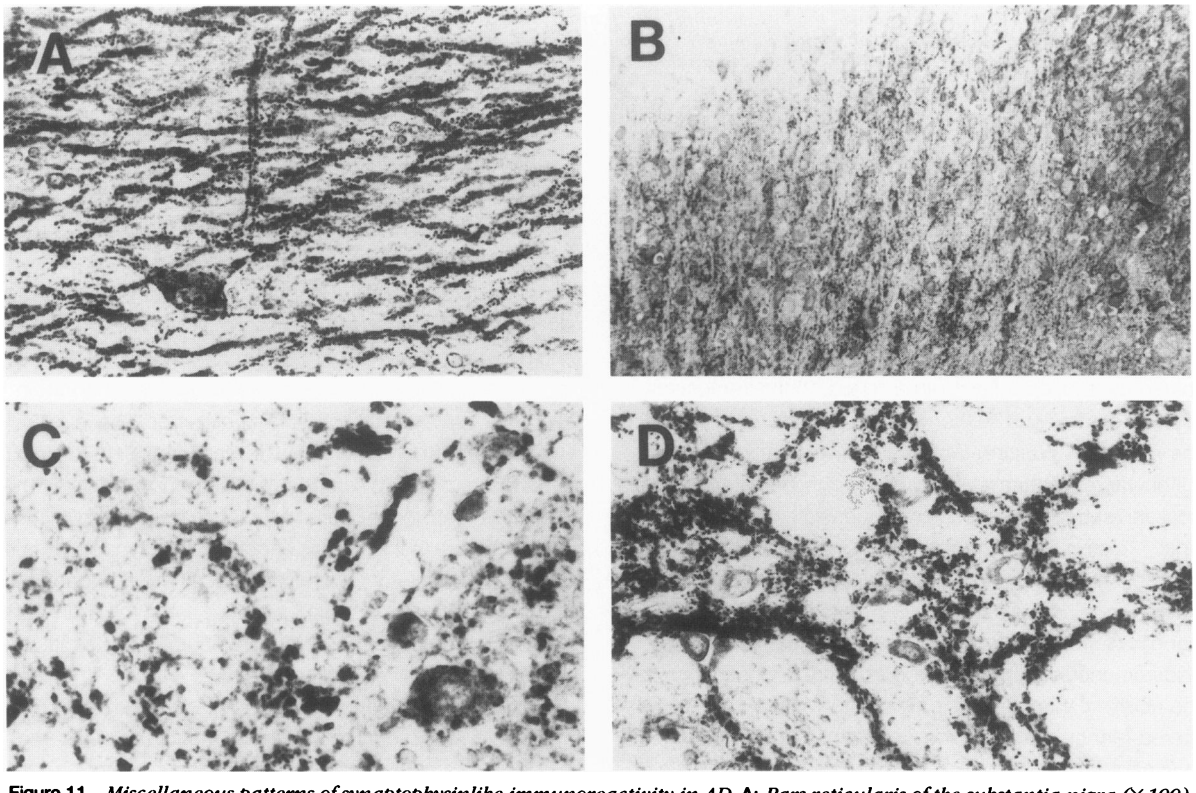

Figure 11. *Miscellaneous patterns of synaptophysinlike immunoreactivity in AD.* **A:** *Pars reticularis of the substantia nigra (×100);* **B:** *lateral geniculate body (×20);* **C:** *oculomotor nucleus (×230);* **D:** *pontine nucleus (×100).*

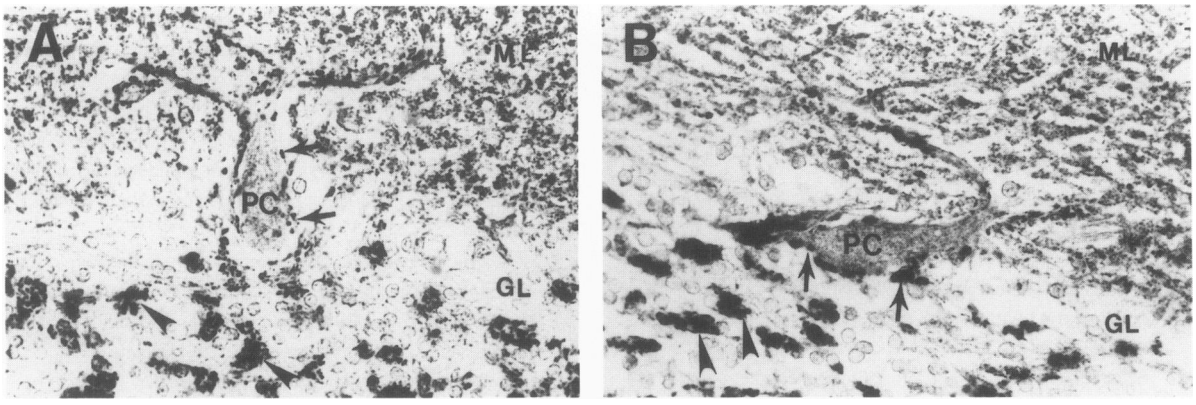

Figure 12. *Synaptophysinlike immunoreactivity of the cerebellar vermis.* **(A)** *In the control cerebellum anti-synaptophysin labeled fine terminals in the molecular layer (ML) as well as terminals (arrows) around Purkinje cels (PC) and the glomerular synaptic complexes (arrow heads) in the granular cell layer (GL).* **B:** *In AD the basic patterns of immunostaining were preserved despite some atrophy (×250).*

different pathologic components of the neuritic plaque.[33] The present study shows that percentage neocortical presynaptic terminal loss is greater than percentage loss of large neurons in the same cortical areas. Interestingly, in this small series of five AD brains and five controls, synapse loss is a more sensitive indicator of the presence of AD than is loss of large neurons. Although large neuron populations are diminished in AD brains relative to controls when large numbers of cases are compared,[8] in this report synapse quantifications show statistically significant differences between AD and controls while large neuron counts do not (Tables 1 to 3). These findings might well be interpreted as implying that synapse loss precedes neuron loss and that the synapse damage is primary rather than a secondary reflection of degeneration occurring in the perikaryon.

Another consistent finding, which may be related to synapse pathology and alteration of the organization of the presynaptic terminals in the AD brain, was the presence of large synaptophysinlike immunoreacting dilated terminals, distributed around amyloid plaques and scattered in cortical and subcortical neuropil. These abnormal terminals are also chromogranin A positive,[34] and some of them have been reported to contain different neurotransmitters.[35] It has been proposed that these plaques originate from degenerating NbM terminals,[36] but studies in the plaque-free AD reticular thalamic nucleus[37] suggest that cortical plaque formation is probably a local process rather than a consequence of NbM degeneration. Electron microscopic studies in the AD neocortex demonstrated that the synapse deficit is associated with a significant increase in the diameter of the synaptic disc in layer V.[14,15] The abnormal immunoreacting neurites scattered in the neuropil in cortical and subcortical areas may correspond to these enlarged terminals. The presence of synaptic vesicle-associated proteins (synaptophysin and chromogranin A) in these abnormal terminals suggests that some of the dystrophic neurites represent regenerating or degenerating presynaptic terminals responding to local synapse damage and loss in the AD neocortex.

References

1. Walaas SI, Jahn R, Greengard P: Quantitation of nerve terminal poupulation: Synaptic vesicle proteins as markers of synaptic density in the rat neostriatum. Synapse 1988, 2: 516–520
2. Masliah E, Terry RD, Alford M, DeTeresa RM: Quantitative immunohistochemistry of synaptophysin in human neocortex: An alternative method to estimate density of presynaptic terminals in paraffin sections. J Histochem Cytochem 1990, 38:837–844
3. Masliah E, Terry RD, DeTeresa RM, Hansen LA: Immunohistochemical quantification of the synapse-related protein synaptophysin in Alzheimer disease. Neurosci Lett 1989, 103:234–239
4. Hamos JE, DeGennaro LJ, Drachman DA: Synaptic loss in Alzheimer's disease and other dementias. Neurology 1989, 39:355–361
5. Wiedenmann B, Franke WW: Identification and localization of synaptophysin, an integral membrane glycoprotein of Mr 38,000 characteristic of presynaptic vesicles. Cell 1985, 41: 1017–1028
6. Jahn R, Schiebler W, Ouiment C, Greengard P: A 38,000-dalton membrane protein (p38) present in synaptic vesicles. Proc Natl Acad Sci USA 1985, 82:4137–4141
7. Hoog A, Gould VE, Grimelius L, Franke WW, Falkmer S, Chejfec G: Tissue fixation methods alter the immunohistochemical demonstrability of synaptophysin. Ultrastruct Pathol 1988, 12:673–678
8. Terry RD, Peck A, DeTeresa R, Schechter R, Horoupian DS: Some morphometric aspects of the brain in senile dementia of the Alzheimer type. Ann Neurol 1981, 10:184–192

9. Lowry OH, Rosebrough NJ, Farr AL, Randall RJ: Protein measurement with Folin phenol reagent. Biol Chem 1951, 193:265–272
10. Peterson GL: A simplification of the protein assay method of Lowry et al. which is more generally applicable. Anal Biochem 1977, 83:346–356
11. Iimoto D, Masliah E, DeTeresa R, Terry RD, Saitoh T: Aberrant casein kinase II in Alzheimers disease. Brain Res 1990, 507: 273–280
12. Laemmli UK: Cleavage of structural proteins during the assembly of the head of bacteriophage T4. Nature 1970, 227: 680–685
13. Towbin H, Staehlin T, Gordon J: Electrophoretic transfer of proteins from polyacrylamide gels to nitrocellulose sheets: Procedure and some applications. Proc Natl Acad Sci USA 1979, 76:4350–4354
14. Davies CA, Mann DMA, Sumpter PQ, Yates PO: A quantitative morphometric analysis of the neuronal and synaptic content of the frontal and temporal cortex in patients with Alzheimer's disease. J Neurosci 1987, 78:151–164
15. Scheff SW, DeKosky ST, Price DA: Quantitative assessment of cortical synaptic density in Alzheimer's disease. Neurobiol Aging 1990, 11:29–37
16. Masliah E, Iimoto D, Saitoh T, Hansen LA, Terry RD: Increased immunoreactivity of brain spectrin in Alzheimer disease: A marker for synapse loss? Brain Res 1990 (In press)
17. Rudelli RD, Ambler MW, Wisniewski HM: Morphology and distribution of Alzheimer neuritic (senile) and amyloid plaques in striatum diencephalon. Acta Neuropathol 1984, 64:273–281
18. O'Kusky J, Colonnier M: A laminar analysis of the number of neurons, glia, and synapses in the visual cortex (area 17) of adult Macaque monkeys. J Comp Neurol 1982, 210:278–290
19. Leclerc N, Beesley PW, Brown I, Colonnier M, Gurd JW, Paladino T, Hawkes R: Synaptophysin expression during synaptogenesis in the rat cerebellar cortex. J Comp Neurol 1989, 280:197–212
20. Difiglia M, Rafols JA: Synaptic organization of the globus pallidus. J Elect Microscop Tech 1988, 10:247–263
21. Gerfen CR: Synaptic organization of the striatum. J Elect Microscop Tech 1988, 10:265–281
22. Girault JA, Raisman-Vozari R, Agid Y, Greengard P: Striatal phosphoproteins in Parkinson disease and progressive supranuclear palsy. Proc Natl Acad Sci USA 1989, 86:2493–2497
23. Walaas SI, Ouimet CC: The ventral striatopallidal complex: An immunocytochemical analysis of medium-sized striatal neurons and striatopallidal fibers in the basal forebrain of the rat. Neuroscience 1989, 28:663–672
24. Goto S, Hirano A, Rojas-Corona RR: Immunohistochemical visualization of afferent nerve terminals in human globus pallidus and its alteration in neostriatal neurodegenerative disorders. Acta Neuropathol 1989, 78:543–550
25. Fagan AM, Masliah E, Terry RD, Gage FH: Synaptophysin-like immunoreactivity in the dentate gyrus of the rat: Response to perforant path transection. Soc Neurosci Abstr 1989, 15: 1389
26. Steward O, Vinsant SL: The process of reinnervation in the dentate gyrus of the adult rat: A quantitative electron microscopic analysis of terminal proliferation and reactive synaptogenesis. J Comp Neurol 1983, 214:370–386
27. Whitson JS, Selkoe DJ, Cotman CW: Amyloid B protein enhances the survival of hippocampal neurons in vitro. Science 1989, 243:1488–1490
28. Roch JM, Sundsmo M, Ward P, Schenk D, Refolo L, Robakis N, Saitoh T: Molecular dissection and functional analysis of the B-protein precursor. Soc Neurosci Abstr 1989, 15:1376
29. Yankner BA, Dawes LR, Fisher S, Villa-Komaroff, Oster-Granite ML, Neve RL: Neurotoxicity of a fragment of the amyloid precursor associated with Alzheimer's disease. Science 1989, 245:417–420
30. Linden DH, Routtenberg A: The role of protein kinase C in long-term potentiation: A testable model. Brain Res Rev 1989, 14:279–296
31. Lovinger DM, Routtenberg A: Synapse-specific protein kinase C activation enhaces maintenance of long-term potentiation in rat hippocampus. J Physiol 1988, 400:321–333
32. Cole G, Dobkins K, Hansen LA, Terry RD, Saitoh T: Decreased levels of protein kinase C in Alzheimer brain. Brain Res 1988, 452:165–170
33. Masliah E, Cole G, Shimohama S, Hansen L, DeTeresa R, Terry RD, Huang KP, Saitoh T: Differential involvement of protein kinase C isozymes in Alzheimer's disease. J Neurosci 1990, 10:2113–2124
34. Munoz DG: Chromogranin A immunoreactivity peptides are major components of neocortical and limbic plaques in Alzheimer disease. J Neuropathol Exp Neurol 1989, 48:378
35. Armstrong DM, Benzing WC, Evans J, Terry RD, Shields D, Hansen LA: Substance P and somatostatin coexist within neuritic plaques: Implications for the pathogenesis of Alzheimer's disease. Neuroscience 1989, 31:663–671
36. Arendt T, Bigl V, Tennstedt A, Arendt A: Neuronal loss in different parts of the nucleus basalis is related to neuritic plaque formation in cortical target areas in Alzheimer's disease. Neuroscience 1985, 14:1–4
37. Masliah E, Terry R, Buzsaki G: Thalamic nuclei in Alzheimer disease: Evidence against the choinergic hypothesis of plaque formation. Brain Res 1989, 493:240–246